prisingly, the theory, being linear and reversible, predicts that an eastward-moving current of constant mass flux should converge into a narrower and more intense jet. As shown in the experiments, catastrophy is avoided in the converging jet because the flow spreads out in the western boundary current to whatever extent is necessary for its eventual convergence as it flows eastward.

(2) With an interior source (or sink) there was an intense recirculation analogous to the effects of the wind-spun vortex described by Munk (1950). The intensity of this recirculation phenomenon was found to be in excellent agreement with a theoretical analysis.

(3) The concepts predicted and verified in SAF were extended to somewhat more complex geometries involving partial radial barriers. An example of such a flow, qualitatively verified by experiment, is shown in figure 16.2, where the indicated transports are the theoretical predictions. Further application to an Antarctic-type geometry illustrated the important role of the radial barriers in allowing the buildup of pressure gradients essential to the maintenance of the geostrophic flow.

(4) In certain source–sink experiments with closed contours of constant fluid depth, it is not possible to construct purely geostrophic regimes of flow. In such cases, lacking resolution of the problem by western boundary currents, the effects of bottom friction dominate the flow. Examples of the complex set of spiral flow patterns necessary in order to transport fluid from an interior source to an interior sink illustrated the dominance of frictional effects.

(5) One feature that would not stand the test of time was the observation of an eastern boundary current when the flow was injected through the eastern boundary of the sector. In later experiments (Faller and Porter, 1976) it was found that this current was probably a density-driven flow due to incomplete thermal control of the injected water.

The analogy between these laboratory experiments and theoretical models of steady wind-driven ocean circulation may be illustrated most clearly by a comparison of the governing equations from three studies. These equations are

Stommel (1948) $\alpha \dfrac{\partial \psi}{\partial x} + \nabla^2 \psi = \gamma \sin \pi y / b,$ (16.1)

Munk (1950) $\beta \dfrac{\partial \psi'}{\partial x} - A \nabla^4 \psi' = \mathrm{curl}_z \tau,$ (16.2)

Faller (1960) $\dfrac{\partial h}{\partial r}\left(\dfrac{1}{r}\dfrac{\partial \psi}{\partial \theta}\right) + \dfrac{D}{2}\nabla^2 \psi$

$= Q - \dfrac{\partial h}{\partial t}.$ (16.3)

In (16.1) $\alpha = (H^*/R)(\partial f/\partial y)$, where H^* is a constant effective ocean depth and R a linear drag coefficient;

and $\gamma = F\pi/(Rb)$, where F is the magnitude of the maximum wind stress per unit mass and b the north-south dimension of the model. In (16.2) A is a horizontal Austausch coefficient, τ the wind stress per unit mass, and ψ' the mass transport stream function. In (16.3) h is the variable fluid depth and Q an internal or surface source of fluid per unit horizontal area.

To illustrate the close correspondence of these equations we may multiply (16.1) by R/H^* and convert the right-hand side to the derivative of a cosine; introduce $\psi = \psi'/H$ as the velocity streamfunction in (16.2), H being the ocean depth; and multiply (16.3) by f/h, reorient the coordinate axes with $r\,d\theta = dx$ and $dy = -dr$, and add the horizontal viscous term. The three equations then become

$$\frac{\partial f}{\partial y}\frac{\partial \psi}{\partial x} \quad + \frac{R}{H^*}\,\nabla^2 \psi \quad = -\frac{1}{H^*}\frac{\partial F \cos \pi y/b}{\partial y},$$

(16.4)

$$\beta \frac{\partial \psi}{\partial x} \quad - A\,\nabla^4 \psi = \frac{1}{H}\mathrm{curl}_z \tau,$$

(16.5)

$$\left(-\frac{f}{h}\frac{\partial h}{\partial y}\right)\frac{\partial \psi}{\partial x} + \frac{fD}{2h}\,\nabla^2 \psi - \nu \nabla^4 \psi = -\frac{f}{h}\,Q + \frac{f}{h}\frac{\partial h}{\partial t}.$$

(16.6)

Equations (16.4)–(16.6) clearly demonstrate the analogy between the laboratory experiment and the basic theories of the steady wind-driven ocean circulation. In particular, $\beta = \partial f/\partial y$ is modeled by $-fh^{-1}\partial h/\partial y$, Stommel's linear drag law corresponds to the Ekman layer effect with R/H^* the equivalent of $fD/2h$, and a positive curl of the wind stress in (16.4) or (16.5) is represented in (16.6) by either an internal (or surface) sink of fluid $-fQ/h$ or by a local rate of increase of depth $(f/h)\partial h/\partial t$. Note also that with the addition of the lateral viscous term to (16.6) this equation is capable of describing steady, linear western boundary currents analogous to those of Munk.

16.5 Experiments with Rotating Covers

The source–sink experiments were more controlled than the wind-driven experiments, and the regular boundary conditions of the 60° sector allowed a clear distinction between the interior flow and the western boundary current (WBC); turbulence was essentially eliminated and the interior flow could be guaranteed to be essentially geostrophic by controlling the flow rates. The introduction of a rotating cover (rotating lid) as the driving mechanism produced a certain degree of additional control by completely enclosing the fluid, by eliminating the possibility of density differences in

Alan J. Faller

the source flow, and by allowing the parameters of the problem to be more easily varied. For example, transient circulations due to an impulsive start of the cover or due to a periodic oscillation of the cover could be easily controlled. Such experiments would be difficult with the sources and sinks of the SAF studies.

Bryan (1960) was perhaps the first to use a rotating lid in an experiment directed toward the understanding of oceanic circulations. Having in mind the planetary waves of the atmosphere and the Gulf Stream meanders, he investigated the baroclinic stability of a two-layer system of salt and fresh water in a 34-cm-diameter cylindrical vessel, the driving force being a slowly rotating lid. He successfully produced symmetric flow, one to three regular waves, and an irregular wave regime, more or less in agreement with a corresponding theory of baroclinic instability. These experiments, of course, had a great deal in common with the annulus experiments of Hide (1958) and with the annulus, open dishpan, and two-fluid experiments of Fultz (1953).

Rotating-lid experiments that turned out to be analogous in many ways to the SAF studies were introduced by Beardsley (1969) in connection with the theories of Pedlosky and Greenspan (1967), the so-called sliced-cylinder model of the wind-driven ocean circulation. The steady-state sliced-cylinder circulation can be described and understood by a relatively simple theoretical analysis, and the following section, through equation (16.18), develops the theory of this model in terms borrowed from the theory of the SAF experiments. This short section will be of particular interest to those directly concerned with the theory of such experiments but may be passed over by the more casual reader. In either case figures 16.3 and 16.4 illustrate the model geometry and circulation.

The radial transport per unit of circumference in the upper Ekman layer due to a differential rotation $\epsilon\Omega$ is simply $T_{Ek}(r) = \epsilon\Omega r D/2$, and the corresponding source strength per unit area for the interior due to Ekman layer divergence is $Q = -\epsilon\Omega d$, independent of radius. For positive ϵ this source is the equivalent of a uniform rise of the free surface in the SAF studies.

At the rim, $r = a$, the Ekman transport $T_{Ek}(a)$ feeds into a Stewartson boundary layer at the circular wall. Since the interior flow is quite slow for large α, little of the flow into the Stewartson layer from above can be taken up by the slow bottom Ekman layer, and we ignore this effect. The Stewartson layer then feeds uniformly into the interior, giving an average flow normal to the wall:

$$U_n = \epsilon\Omega a D/2h. \qquad (16.7)$$

The interior geostrophic flow is governed by equation (16.6) omitting the lateral and bottom friction
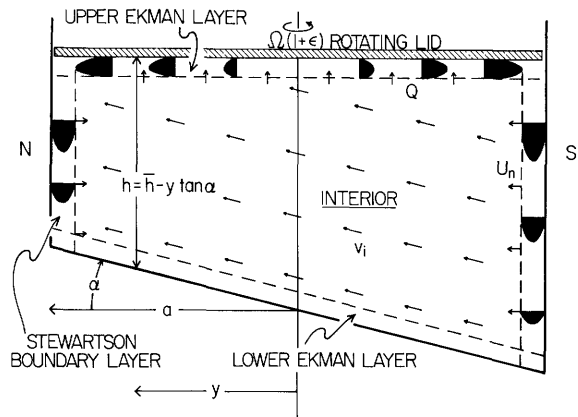

Figure 16.3 A schematic N–S cross section of the circulation in a sliced-cylinder model. The circulation is driven by the divergent Ekman layer of the rotating lid with the induced suction velocity $Q = -\epsilon\Omega D$. The Ekman flow at the rim of the rotating lid turns into the Stewartson layer and feeds the interior as a velocity component normal to the wall U_n. The geostrophic S–N interior flow v_i is independent of x and y and is given by $v_i = -Q/\tan\alpha$. Global continuity of mass is satisfied by geostrophic east–west interior flows and the western boundary current (not shown).
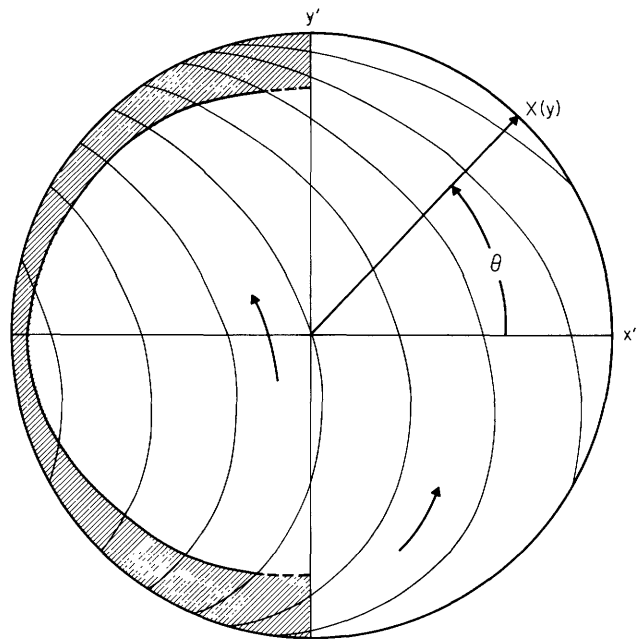

Figure 16.4 Streamlines of the theoretical, linear, steady-state circulation in the sliced-cylinder experiment of Pedlosky and Greenspan (1967) and Beardsley (1969) for a bottom slope angle $\alpha = 30°$. For large α the flow away from the eastern boundary becomes evident in the streamline pattern because of the reduction of v_i in comparison to U_n (figure 16.3). The variation in width of the western boundary current is schematically illustrated.

terms. The resultant equation for the south-to-north interior flow is

$$v_1 = -Q/\tan\alpha = \epsilon\Omega D/\tan\alpha, \tag{16.8}$$

where $v_1 = \partial\psi/\partial x$ and $\tan\alpha = -\partial h/\partial y$. Thus for $\epsilon > 0$, as in the case considered by Pedlosky and Greenspan (1967), $Q < 0$ (Ekman suction) and it follows that $v_1 > 0$. Later experiments of Beardsley used $\epsilon < 0$.

The interior velocity component u_1 is determined by continuity. For a cell in the interior mass continuity is given by

$$\left[v_1 h - \left(v_1 h + \frac{\partial v_1 h}{\partial y}\,dy\right)\right]dx$$

$$+ \left[u_1 h - \left(u_1 h + \frac{\partial u_1 h}{\partial x}\,dx\right)\right]dy + Q\,dx\,dy = 0.$$

Using equation (16.8) and $\partial h/\partial x = 0$ it is readily found that $\partial u_1/\partial x = 0$. Following the assertion made in SAF that there can be no geostrophic flow component normal to the eastern boundary, but that unlimited flow into or out of the western boundary layer is permitted, the value of u_1 is determined by u_e, the west-east flow at the eastern boundary. This in turn is composed of two parts: the source flow from the Stewartson layer is $u_{e1} = -U_n/\cos\theta = -\epsilon\Omega Da/2h\cos\theta$; and from the constraint that there be no geostrophic flow normal to the boundary we obtain $u_{e2} = -v_1\tan\theta$. The total west-east interior flow is then

$$u_1 = -\epsilon\Omega D\left(\frac{a}{2h\cos\theta} + \frac{\tan\theta}{\tan\alpha}\right). \tag{16.9}$$

Integrating (16.8) and (16.9) to obtain an interior streamfunction defined by $v_1 = \partial\psi/\partial x$ and $u_1 = -\partial\psi/\partial y$ gives

$$\psi' = \frac{\psi}{\epsilon\Omega Da} = \frac{a}{\bar{h}}\frac{\sin^{-1}y'}{2}$$

$$+ \left[\left(\frac{a}{\bar{h}}\right)^2\frac{\tan\alpha}{2} + \frac{1}{\tan\alpha}\right][1 - (1 - y'^2)^{1/2}]$$

$$+ \frac{x'}{\tan\alpha}, \tag{16.10}$$

where $y' = y/a$, $x' = x/a$, and $\psi' = 0$ at $x' = 0$, $y' = 0$. In this integration I have used the approximation

$$h = \bar{h} - y\tan\alpha \cong \bar{h}\left(1 + \frac{y\tan\alpha}{\bar{h}}\right)^{-1},$$

and as a result (16.10) differs slightly from Beardsley's (1969) equation for pressure.

Figure 16.4 illustrates the pattern of ψ' for $\alpha = 30°$. With this large slope v_1 is small and the effect of the source at the rim is made conspicuous [compare Pedlosky and Greenspan (1967, figure 5)]. Since the rim source does not directly contribute to the north-south

(N-S) transport, it is easily seen, as pointed out by Beardsley (1969), that the WBC transport T_w is determined solely by the value of v_1 integrated over x. By continuity

$$T_w(\text{N-S}) = -\int_{-X(y)}^{X(y)} hv_1\,dx = -2hv_1X(y). \tag{16.11}$$

The WBC transport parallel to the boundary, however, requires that the result in (16.11) be divided by $\cos\theta$. Dividing also by $\epsilon\Omega Dah$, the nondimensional transport per unit depth and parallel to the boundary is

$$T'_w(||) = \mp 2\tan\alpha, \tag{16.12}$$

the upper sign corresponding to $\epsilon > 0$.

But although $T'_w(||)$ is constant, the current sees different variations of depth $\partial h/\partial s$ along its axis s, and the width of the current must change. For positive y (and $\epsilon > 0$ as in figure 16.3) the current narrows as it moves south toward $y = 0$, and it is also fed from the interior flow. For $y < 0$ the current feeds the interior and at the same time broadens because $\partial h/\partial s$ decreases along the direction of flow. By the time the flow reaches $\theta = -\pi/2$ the WBC must completely disperse, and under these circumstances it is not surprising that an instability occurs for sufficiently large ϵ.

The steady-state, linear analysis given above cannot take into account transients, instabilities of the flow, details of the boundary layer flow, or the range of validity of the theory. These aspects of the problem were the principal focal points of the analytic, numerical, and experimental sliced-cylinder studies cited above. Nevertheless, the simplified treatment given here reveals the essential physical mechanisms without mathematical obfuscation. In this spirit we continue with an elementary treatment of the WBC to illustrate certain principles analyzed by Beardsley (1969) and later disucssed also by Kuo and Veronis (1971).

Beardsley noted that when the angle α is small, the WBC is dominated by bottom Ekman-layer pumping, rather than by lateral friction. Except very close to the wall, the boundary current then is essentially that found by Stommel (1948) with friction entering the problem through a constant drag coefficient R/H^*, as in (16.4).

Figure 16.5 illustrates a WBC profile, the cross-stream Ekman transport beneath the current, and the vertical flux from the Ekman layer. The WBC is normally much wider than D, and in the case where lateral friction dominates the boundary layer, the ratio of its width W' to D is $W'/D = (h/D)^{1/3}(4/\tan\alpha)^{1/3}$ (see below). Thus, in the Ekman layer the usual boundary-layer assumption applies, namely, that lateral variations of the flow can be neglected in comparison to variations normal to the boundary. Under the simplifying as-
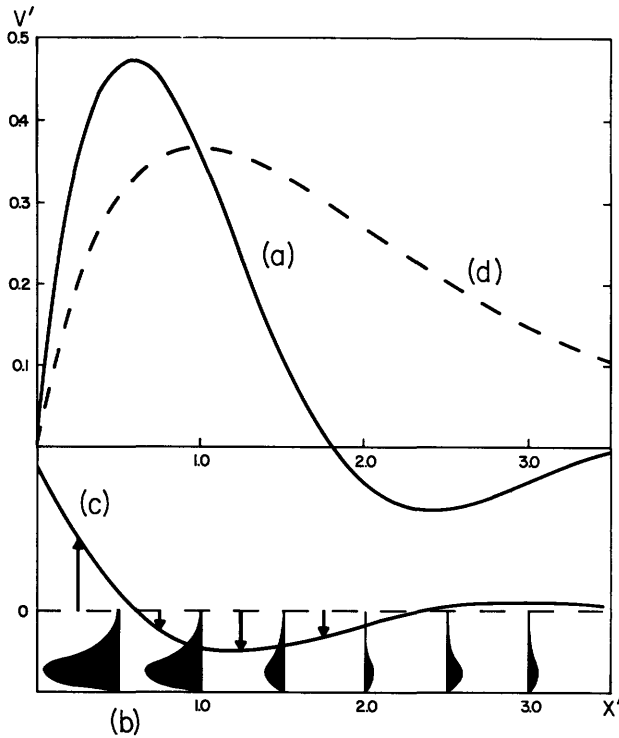
Alan J. Faller

Figure 16.5 The nondimensional velocity component $v' = e^{-x'} \sin \sqrt{3}x'$ for the Munk boundary layer in which lateral friction dominates the vorticity balance. (b) The Ekman transport beneath the boundary layer in (a). (c) Flux into or out of the western boundary current by Ekman layer convergence or divergence. (d) The nondimensional velocity $v^* = x^*e^{-x^*}$ at the transition between the Munk and the Stommel boundary layer regimes.

sumptions given below it can also be shown that the Ekman layer transport is proportional to the local value of v above the Ekman layer. An inconsistency, apparent in figure 16.5, is that the maximum Ekman layer pumping occurs at $x = 0$ and the no-slip condition at the wall is not satisfied. To completely justify the approximate analysis given below, a more complete boundary-layer scaling and analysis including the sidewall Stewartson layers, as given by Beardsley (1969) and Kuo and Veronis (1971), is required.

Here we specify a total northward transport of the WBC, T_w, a straight N-S boundary, a linear depth variation $-\partial h/\partial y = +\tan \alpha$, and a locally constant depth, where h appears as a coefficient in the final differential equation; and we neglect variations of the current with y, i.e., along the boundary. Then (16.6) is appropriate, and after dividing by v it reduces to the third-order, ordinary linear differential equation with constant coefficients

$$\frac{d^3v}{dx^3} - \left(\frac{1}{Dh}\right)\frac{dv}{dx} - \left(\frac{2\tan\alpha}{D^2h}\right)v = 0 \qquad (16.13)$$

subject to the conditions $v = 0$ at $x' = 0$, $v = 0$ at $x' = \infty$, and $T_w = \int_0^\infty vh\,dx$. It is convenient to define a

nondimensional coordinate $x' = x/W'$, where $W' = [8\ hD^2/(2\tan\alpha)]^{1/3}$ will be seen to be the characteristic width of the WBC. Then, temporarily neglecting the Ekman layer effect by setting $D = 0$, (16.13) reduces to

$$\frac{d^3v}{dx'^3} - 8v = 0. \qquad (16.14)$$

After applying the boundary conditions the solution to (16.14) is the exponentially-damped sine profile

$$v = \left(\frac{4}{3^{1/2}}\frac{T_w}{hW'}\right)e^{-x'}\sin\sqrt{3}x', \qquad (16.15)$$

which corresponds to the oscillatory solution of Munk (1950). A nondimensional v' for this result is plotted in figure 16.5.

The WBC in the absence of lateral friction has been called the *Stommel boundary layer* (Kuo and Veronis, (1971), and from (16.13) this is given by the solution to

$$\frac{dv}{dx} + \frac{2\tan\alpha}{D}v = 0. \qquad (16.16)$$

Here the condition $v = 0$ at $x = 0$ must be relinquished, and the condition at infinity will be satisfied automatically. Applying the transport condition, the solution is the exponential profile

$$v = \frac{T_w}{hW''}e^{-x''}$$

where

$$x'' = x/W'' \quad \text{and} \quad W'' = (D/(2\tan\alpha)).$$

In terms of a simulated β-effect, being given $\beta^* = (-2\Omega/h)(\partial h/\partial y)$ it follows that $W'' = \Omega D/h\beta^*$.

With the scaled coordinate x', the full equation is

$$\frac{d^3v}{dx'^3} - B\frac{dv}{dx'} - 8v = 0, \qquad (16.17)$$

where $B = 4(D/h)^{1/3}(2\tan\alpha)^{-2/3}$. Substituting the trial solution $v = e^{kx}$, the characteristic equation is

$$k^3 + ak + b = 0, \quad \text{where} \quad a = -B \text{ and } b = -8.$$

Complex values of k correspond to oscillatory solutions, and nonoscillatory boundary layers occur only for $(b^2/4) + (a^3/27) \leq 0$, or $D/h \geq 27\tan^2\alpha$. Accordingly, the condition $D/h = 27\tan^2\alpha$ may be defined as the transition point between the Munk and Stommel boundary layer regimes. In the SAF and F experiments where $\tan\alpha = \Omega^2r/g$ this transition took place at approximately $r = 23$ cm in a tank of radius $a = 100$ cm.

The solution at this transition is the product of linear and exponential functions as given by

$$v = \left(\frac{T_w}{hW^*}\right)x^*e^{-x^*}, \qquad (16.18)$$

where $x^* = x/W^*$ and $W^* = (3hD/4)^{1/2}$. The slope $\tan \alpha$ is implicit in this expression for W^* through $D/h = 27 \tan^2 \alpha$.

The theoretical studies of Pedlosky and Greenspan (1967) for the sliced-cylinder geometry emphasized the transient Rossby-wave character of the spin-up problem, i.e., the development of the steady-state flow by the accumulated effect of westward-propagating Rossby waves in response to the spin-up of the lid. Owing to the need for a more detailed examination of the steady-state flow and because of the discovery of an instability of the WBC, Beardsley's original experiments were temporarily diverted from the goal of studying the transient response. The instability was analyzed in detail by Beardsley and Robbins (1975), who described it as a "*local* breakdown of the finite-amplitude topographic Rossby wave embedded in the western boundary current transition region." This general description would seem to fit almost any reasonable theory of the observed instability, but it is noteworthy that a plausible analytical theory was presented and that numerical calculations of the flow showed similar instabilities and good agreement with the experiments.

In a companion paper Beardsley (1975) experimentally and theoretically examined the transient response of the flow to an oscillatory rotation of the lid. He again found good agreement between theory and experiment in the resonant response of topographic Rossby wave modes. In addition he found that the Stokes drift associated with the Rossby waves partially offset the mean Eulerian flow, a consideration of possible importance for the interpretation of oceanic processes (the result generally agrees with the theory of Moore, 1970). In a short series of trial experiments, Beardsley (1974) also changed the geometry of his experiment by replacing the planar sloping bottom with an axisymmetric conical bottom and introduced partial radial barriers, analogous to those of F (1960), to simulate certain aspects of the Antarctic circulation regime. These experiments again clearly illustrated the anticipated steady-state interior and boundary-layer flows.

Another interesting class of rotating-lid experiments was introduced by D. J. Baker. Baker and Robinson (1969) have presented a comprehensive theoretical and experimental analysis of the results and Baker (1970) has given a more pictorial and descriptive account of this research for popular consumption. The fluid (a solution of thymol blue) was contained, top and bottom, between spherical boundaries ground from plastic blocks. The lateral boundary was a circular cylinder, and the lower boundary was rotated to generate the flow. The confined fluid was meant to represent a circular ocean of uniform fluid on a spherical earth. This ingenious apparatus was mounted on a rotating table

in such a way that the center of the model ocean could be set for any latitude from the equator to the pole. Indeed, the primary purpose of this experiment was a study of equatorial dynamics in the hope of obtaining a uniform-fluid analogue of the equatorial undercurrent.

Baker (1966) had introduced an important new quantitative method for the measurement of slow flows in the interior of liquids, the thymol-blue-indicator technique. A slightly acidic solution of thymol blue is used as the working fluid, and platinum wires are strung through the interior. When a current is passed through the wires the indicator immediately adjacent to the wires turns to a bluish-brown color and serves as a tracer for the subsequent flow. Baker and Robinson (1969) used an extensive rectangular array of wires to illustrate and measure the overall pattern of flow for a considerable range of flow speeds.

In the range of Rossby numbers where steady laminar flow would be expected, the basic interior and boundary-layer circulations were as would be anticipated from elementary theory. At higher values of the Rossby number, however, interesting asymmetries and irregularities of the flow, attributable to inertial effects, were observed.

When the latitude of the center of the model ocean was sufficiently close to the equator that a large equatorial zone was present, an interior zonal current opposite to the direction of driving of the cover was observed, and this current was tentatively identified as a uniform fluid analogue of the equatorial undercurrent.

16.6 A Variety of Interesting Experiments

16.6.1 Further Source–Sink Experiments
Kuo and Veronis (1971) reinvestigated many of the SAF and F experiments with a similar configuration of the apparatus but with a number of interesting variations and with a more exacting theoretical analysis of the boundary-layer flow. Their principal observational tool was the thymol-blue technique of Baker (1966) except that the platinum wires were alternately coated and exposed in short strips so that a pulse of electric current gave a dashed line of dye. This method allowed more accurate measurements of the flow components and improved the flow visualization.

As in the studies of Beardsley (see section 16.5) their experimental conditions covered both the Munk and Stommel WBC regimes and their experimentally observed current profiles were in excellent agreement with theory.

In addition to the effect of the paraboloidal free water surface, depth variation was controlled by a sloping bottom, and in one case by a partially sloping bottom in the SW corner of the 60° sector. The latter experiment was used to confirm certain basic theories about

Alan J. Faller

the effect of bottom topography on the separation of the boundary current from the coast. Concentrated sources and sinks in the interior, similar to the source used in F (1960) and to the effect of the wind-spun vortex of Munk (1950), also illustrated separation of the boundary current because of the source–sink distribution.

Veronis and Yang (1972) extended the uniform fluid WBC theory and experiments to cases with significantly nonlinear flow. Once again, the theoretical predictions, including both lateral viscous and Ekman layer effects, were accurately verified in the experiments. Some unsuccessful attempts were made to produce a sufficiently rapid and narrow western boundary current for barotropic instability.

16.6.2 A Two-Layered Model
A major innovation and advance in laboratory modeling has recently been achieved by Krishnamurti (Krishnamurti and Na, 1978; Krishnamurti, 1978) by the introduction of controlled rotating-lid experiments with a two-layer system having no closed contours of depth. Using a conical bottom and a rotating conical lid, radial depth variations are produced in both the upper and lower layers. Under conditions that would be stable for a uniform-fluid experiment, the two-fluid experiment produces baroclinic instability and a number of interesting features associated with the deformation of the interface of the two fluids. Perhaps the most striking of these features is the upwelling of the lower fluid to the "surface" at the western boundary and the concurrent separation of the WBC, a phenomenon predicted by Parsons (1969) (see chapter 5).

Together with the laboratory experiments, Krishnamurti (1978) has theoretically evaluated the comparative spin-up times of the ocean and laboratory models in terms of the Rossby radius of deformation in relation to the fluid depth. These considerations suggest that the two-fluid experiments will have a number of interesting applications.

16.6.3 Flow over Sills and Weirs and through Straits
Smith (1973, 1977) was concerned with the flow of cold bottom water after it had passed through the Denmark Strait from the Norwegian Sea. This is a problem concerning effects of friction and sloping bottom on the modification of a baroclinic current system. To accompany a theoretical model of bottom frictional effects, Smith developed a laboratory experiment in which denser fluid was drained slowly through a source tube onto the sloping bottom of a rotating tank. He observed a variety of systematic wavelike and eddy-like oscillations of the flow that were found to be consistent with appropriate theories of baroclinic instability. In the 1977 paper he compared his experimental results

with observations of the pulsed flow over the sill in the Denmark Strait, and he concluded on the basis of the significant nondimensional numbers that the natural case should correspond to what he described as "the meandering jet, vortex train variety (Class I)." Experiments of this type indeed represent a sophisticated application of laboratory experiments to our understanding of detailed oceanic phenomena.

Flows through straits and over sills have been of great interest in a wide variety of nonrotating systems, and engineering data characterizing these flows have long been available. In oceanic applications, however, the Coriolis force must play an important role in modifying or controlling the flow, and from experience with topographic β-effects one might also expect the detailed geometry to be of great significance in many cases. An obvious oceanographic example of restricted flow is that through the Straits of Gibraltar, but many other examples may also be mentioned, such as the seepage of Antarctic Bottom Water through small gaps in the Mid-Atlantic Ridge.

The experiments of Whitehead, Leetmaa, and Knox (1974) and of Sambuco and Whitehead (1976) have been concerned with problems of this type, approaching them experimentally beginning with the nonrotating system and gradually increasing the effect of rotation. Their studies may be characterized as being concerned chiefly with the restriction of the volume transport of the lower fluid through the strait, or over the sill, at relatively high Rossby numbers. Smith's studies, in contrast, have been concerned primarily with very low Rossby numbers, and with frictional effects on sloping boundaries after the flow has left the constriction.

16.6.4 The Generation of Mean Flows by Turbulence
One of the more elaborate and more significant recent laboratory studies has been that of Colin de Verdière (1977), who examined the response of a rotating fluid in various geometries to Rossby waves generated by a complex pattern of oscillatory sources and sinks of fluid introduced through holes in the bottom of the tank. He considered three cases: an f-plane model (constant depth); a polar β-plane model with a depth variation from the paraboloidal shape of the free surface and with closed height contours; and a sliced-cylinder model. Comparing turbulence and wave theory with the complex flow patterns of his experiments, he included in his studies the interaction of two-dimensional turbulent eddies for a fluid with energy sources and sinks, the evolution of the flow toward statistical equilibrium, and the interaction of Rossby waves with a mean flow.

The extent and variety of the experiments covered by Colin de Verdière preclude a detailed exposition of all his results, but in general it may be said that the theoretical expectations, based upon the theories of

potential vorticity mixing of Rhines (1977), were experimentally verified. By way of example, we mention here the results of a polar β-plane experiment in which the flow was driven by alternating sources and sinks of fluid at the outer boundary. This complex system was arranged to produce a westward-moving Rossby wave. Through the preferential inward (northward) diffusion of anticyclonic vorticity, the Rossby wave in effect transferred energy to a westward mean flow north of its region of generation. When the forcing was turned off and the flow was allowed to decay, measurements of the mean flow and of the perturbation kinetic energy indicated that the eddies continued to feed energy into the mean flow.

The particular results given above concerning the generation of mean flows by turbulence in a β-plane model were anticipated by the experiments of Whitehead (1975), who excited turbulent motions in a somewhat different manner. Whitehead used a 2-m-diameter cylindrical tank and vertically oscillated a circular horizontal plastic disk within the fluid, the disk being 20 cm in diameter and centered at 66 cm radius. By thus driving turbulence and Rossby waves with no direct input of angular momentum, it was clear that the observed mean flow [eastward at the latitude (radius) of the oscillator, and westward to the north and south] was due to the lateral redistribution of angular momentum by the waves and turbulence. In such experiments, however, it is difficult to be certain that the mechanical apparatus is not partially forcing the mean flow. Suppose, for example, that the vertical axis of the oscillating plate were tilted by 1° one way or the other. Would this have an influence upon the generation of the mean flow, and if so, how much? The experiments of Colin de Verdière, using sources and sinks parallel to the rotating axis, do not seem to be subject to the same possible difficulties, but one must be very cautious in experiments of this type.

It is interesting to note that the late Professor V. P. Starr (of Chicago and MIT) probably had a significant influence upon these studies, for Whitehead acknowledges many interesting conversations with Starr and his students. I note this fact particularly because it was at the suggestions of Professors Starr and Rossby that Fultz began his experimental studies at the University of Chicago, and one of the original intentions of those studies was an examination of exactly the problem discussed above. The experiments of Fultz eventually centered upon thermally driven circulations in a hemispherical shell, but Starr (personal communication, circa 1952) always kept in mind the possibility of locally pulsing one of the spherical shells to generate purely mechanically driven circulations without the direct introduction of a mean flow.

The experiments discussed above appear to be contradicted by an experiment of Firing and Beardsley (1976), who generated an isolated eddy in a sliced-cylinder experiment. It was found that the total nonlinear effect of the eddy was the generation of cyclonic vorticity in the northern portion of the basin and anticyclonic vorticity to the south. The net effect was explained as the result of the competition between two opposing tendencies:

Potential vorticity conservation which imparts negative vorticity to northward moving water columns and positive vorticity to southward moving columns, and relative vorticity segregation which gives water columns with positive relative vorticity a tendency to move north and those with negative vorticity a tendency to move south. Thus the positive circulation induced in the northern half of the basin by the dispersing eddy indicated the dominance of the vorticity segregation mechanism in this flow.

There is need for further theoretical and experimental studies to rationalize the apparent differences between these results and those of Colin de Verdière (1977) and Whitehead (1975). The experiment of Firing and Beardsley was conducted in a system with no closed geostrophic contours and with an isolated eddy as the disturbance. The other experiments had continuous sources of Rossby waves or turbulence in an open circular tank without meridional barriers and therefore without the possibility of western boundary current and Rossby-wave reflection from meridional barriers.

16.6.5 The Generation, Propagation, and Reflection of Rossby Waves

Topographically generated Rossby waves were studied in detail by Long (1951) for the flow between hemispherical shells. Since that time many experimenters have generated stationary Rossby-wave patterns by the flow over a ridge or obstacle, using the radial depth variation to produce the simulated β-effect. Stationary Rossby waves have also appeared in a variety of experiments where the flow was obliged to separate from the western boundary and the boundary current was sufficiently nonlinear.

Ibbetson and Phillips (1967), however, were the first to investigate the generation, propagation, and reflection of Rossby waves specifically in an oceanographic context. In their classic paper they experimentally studied the free propagation and dissipation of Rossby waves from an oscillating-paddle wave generator (figure 16.6). Moreover, they developed a simple theory and a companion experiment for damped oscillatory flow in the closed region between their oscillating paddle and a radial barrier to the west. For a specific paddle frequency their theoretical solution consisted of the sum of two waves of the same frequency that could be identified as the one generated in the east by the paddle
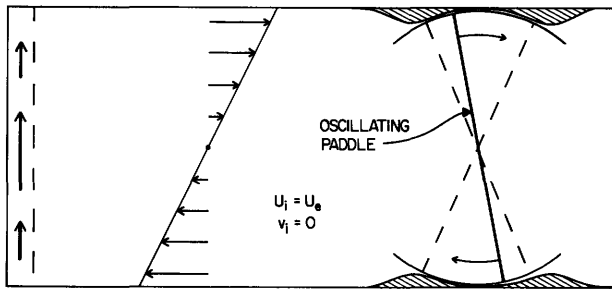
Figure 16.6 A schematic representation of the Ibbetson and Phillips (1967) experiment for the limiting case of zero frequency of the oscillator. The interior currents are then purely zonal with speeds v_i equal to the speed of the eastern boundary u_e. The steady-state western boundary current transport is determined by continuity as in the SAF (1958) experiments.

and its reflection from the western boundary. Since the reflected wave was of high wavenumber and large amplitude, its energy was subject to rapid dissipation as it progressed eastward from the boundary. The net result was a strong concentration of radial motions in the vicinity of the western boundary.

The application of these results to steady-state ocean-circulation theory, as well as to the transient oscillations, becomes evident when one lets the driving frequency of the paddle approach zero. This condition is illustrated in figure 16.6. From section 16.5, because there are no interior sources and sinks of fluid, the interior radial velocity is $v_i = 0$. It also follows that $u_i = u_e$, where u_e is the zonal velocity of the eastern boundary, which in this case is the velocity of the paddle. The wave generated by the paddle thus degenerates to purely east–west currents, and the reflected wave, with very high longitudinal wavenumber and very large radial flow, in the limit becomes the western boundary current.

16.6.6 Simulation of the American Mediterranean

An account of laboratory models of ocean circulation would not be complete without a brief discussion of Ichiye's (1972) laboratory studies of flow in the Gulf of Mexico and the Caribbean Sea. These were attempts to reproduce the known circulations insofar as is possible with a uniform fluid, by detailed scaling of the complex coastlines and bottom topography. The avowed purpose was "to understand the effects of bottom and coastal configuration of the two seas on the geostrophic current of barotropic mode. The vertical structure of the flow and the details of the horizontal current patterns are not a subject of this study."

Two separate model systems were constructed: one for the Gulf of Mexico, driven by a source of forced inflow through the Yucatan Straits, and outflow through the Straits of Florida; the other, of the Carib-

bean Sea and adjacent portions of the Gulf and the Atlantic Ocean, driven by a pattern of winds from fans. Rossby numbers and Reynolds numbers of the flow were varied to discover how the overall patterns of flow and the various cyclonic and anticyclonic vortices would respond to different values of these parameters.

In summary it may be said that many realistic features of the natural circulations were reasonably well reproduced, for example, the distribution of geostrophic mass transport in the Caribbean; but other features, notably the major current systems in the Gulf, were unacceptable. Of course, one of the values of experiments of this type lies in failure, for we are then directed to inquire about the specific sources of error. In this study it is likely that density stratification, or at least a two-layer system, may be necessary for greater realism of the model circulations. With the strong topographic effects that must be important in these nearly enclosed basins, the normal β-effect may be negligible, and a stratified-fluid experiment may be practical.

16.6.7 A Laboratory Study of Open-Ocean Barotropic Response

The above title is that of Brink (1978), who studied the f-plane and β-plane response of a rotating fluid with a free surface to applied surface-pressure oscillations. A problem of direct interest is the response of the world oceans to atmospheric pressure fluctuations of all scales (see chapter 11). In the absence of the planetary and topographic β-effects, the f-plane response should follow the inverse barometric effect except for frequencies close to resonance with inertia-gravity waves. When near resonance occurs there may be significant overshoot, i.e., excess amplitude response compared to the inverse barometer effect. With the β-effect there can be significant undershoot because of the propagation of Rossby waves, although if the scale and frequency of the pressure fluctuations should correspond to one of the normal modes of oscillation of the basin, there again could be significant overshoot.

In his β-plane experiments, Brink oscillated the air pressure over an enclosed region bounded by circular arcs at 15.2- and 30.5-cm radius and by radial walls separated by 120° of azimuth. With the tank radius of 42 cm, the area of forced-pressure oscillation comprised about 13% of the total surface area. The pressure vessel was designed to just touch the water surface with the intent of not seriously interfering with the water circulation or the propagation of waves. Measurements of the water-level response were obtained with capacitance height gauges.

Approximate theoretical solutions for the response of the water level were compared with the amplitudes and phases of the observed height variations at several

475
Laboratory Models of Ocean Circulation

sites. Reasonable agreement was found in many cases. The most serious lack of agreement occurred at the higher frequencies, and this was tentatively attributed to the use of a primitive (steady-state) Ekman-layer model for viscous damping, rather than one that took into account transients in the Ekman layer. Brink concluded that departures from the inverse barometer effect are to be expected due to propagating free modes of oscillation as predicted by theory.

16.6.8 Gulf Stream Rings

A laboratory study that may have direct analogy to the ocean was that of Saunders (1973), who experimentally tested the stability of a two-layer baroclinic vortex. While this experiment was similar in certain respects to the baroclinic instability studies of Fultz (1953), Hide (1958), Bryan (1960), Hart (1972), and others, Saunders pursued an interesting analogy with the stability of Gulf Stream Rings and other isolated oceanic vortices.

A cylindrical column of denser fluid was released within a lighter fluid, the entire system being initially in solid-body rotation. The lower part of the denser fluid spread out rapidly, leading to a low-level anticyclonic vortex and an upper-level cyclonic vortex. The increase in radius at the bottom $R - R_0$ from the initial radius of the cylindrical column R_0 was approximately equal to $\lambda = (g'H)^{1/2}/f$, the Rossby radius of deformation, where $g' = g\,\Delta\rho/\rho$, $\Delta\rho$ is the difference in fluid densities, H the fluid depth, and f the Coriolis parameter.

Defining the parameter $\theta = \lambda^2/R_0^2$, it was found that for $\theta < 1$ the initial circular vortex was unstable and would break up into a number of smaller vortices, each having $\theta > 1$.

Calculation of an equivalent value of θ for two stable Gulf Stream rings gave $\theta \approx 2$. Thus the stability or instability of the laboratory vortices and the corresponding stability characteristics of Gulf Stream rings, or other nearly circular oceanic vortices, may represent one of the most unambiguous tests of baroclinic instability in the ocean.

Two items that may be of historical interest in connection with these experiments are the following. First, in studies designed to test the bubble theory of cumulus convection Saunders used a small, hemispherical volume of buoyant fluid released at the bottom of a large and deep tank of water. Turned upside down, a small volume of dense fluid was released and allowed to fall, expanding as an entraining spherical-cap bubble. Saunders noticed that when the falling dense fluid impinged upon a rigid boundary it spread out somewhat analogously to an atmospheric squall line, and a series of experiments in a shallow fluid were undertaken. Since von Arx's old rotating turntable was available in the same laboratory, extension of these experiments to

the rotating system was quite practical without the construction of new elaborate apparatus. Saunders first performed these rotating experiments in 1963 and the critical parameter for the stability of this type of vortex in fact was determined well before the extent and significance of Gulf Stream rings were fully appreciated.

The second item of interest is that in the late summer of 1954, when this author was first using von Arx's apparatus for atmospheric model studies, H. Stommel and W. V. R. Malkus one day suddenly appeared in the laboratory equipped with huge jugs of xylene and carbon tetrachloride (which at that time were not known to be so dangerous). Their intention was almost exactly the experiment later performed by Saunders, namely, to release a cylindrical column of a dense mixture of their two fluids in the center of a rotating tank full of water. They were specifically interested in relating the radial spread of this column of dense fluid to the Rossby radius of deformation, which had recently been recognized as an important parameter. Unfortunately this combination of liquids would have dissolved the sealer cementing together the base and rim of the tank. How might the history of laboratory studies have been altered in its course had this author allowed them to proceed with their experiment?

16.6.9 Spin-Up

Laboratory experiments and the theory of spin-up of a rotating fluid began with the work of Stern (1959, 1960b). In the former (unpublished) paper he presented the basic theory of spin-up and a description of laboratory experiments that accurately verified the predicted spin-up times as well as the integrated radial and tangential displacements of floating tracer particles. In the latter paper an instability of Ekman flow was postulated as the source of disagreement between the experiments and laminar theory in certain cases. In more recent experiments, also with a uniform fluid, Fowlis and Martin (1975) used a laser Doppler velocimeter and found clear evidence of the elastoid-inertia oscillations to be expected from transients in the Ekman layer owing to the abrupt change in rotation rate (Greenspan and Howard, 1963). In the wind-driven ocean, however, the stratification may drastically alter the spin-up characteristics from what would be anticipated for a uniform fluid.

Stratified spin-up experiments (e.g., Buzyna and Veronis, 1971; Saunders and Beardsley, 1975) generally have been conducted in the same manner as the classical uniform fluid cases—with an abrupt change in the rotation rate. In such a case, all natural modes of oscillation can be excited, and as a result it has been difficult to match satisfactorily theory and experiment. In recent studies by Beardsley, Saunders, Warn-Varnas, and Harding (1979), however, the spin-up was made

gradually, thus avoiding the excitation of high-frequency oscillations. As a result, substantially better agreement than in previous experiments was found between a simple quasi-geostrophic numerical model and observations of the response of the interior temperatures and the azimuthal velocities.

16.6.10 Langmuir Circulations
One of the areas of research in which H. Stommel played an early role was the study of windrows—slicks on a natural water surface oriented in streaks along the wind direction. In a series of approximately 200 observations on Ashumet Pond, Cape Cod, Massachusetts, over the 7-month period May–November 1950, Stommel (1952) observed the presence or absence of surface streakiness parallel to the wind, and he attempted to relate the occurrence of streaks to various meteorological factors including the wind, cloudiness, humidity, and the air–water temperature difference as a measure of the thermal stability. The single parameter that seemed to be related to the occurrence of streaks was the wind speed, and table 16.1 is a summary of Stommel's data. The occurrence of streaks is clearly seen to be dependent upon the wind speed, and streaks often were observed at speeds much less than what is now generally considered to be the critical value, about 3 m s^{-1} (Walther, 1966).

These data do not seem to indicate a sharply defined critical speed, and the apparent critical speed given by other observers should perhaps be questioned in view of the facts that the observation of streakiness is a subjective one, the amount of surface material present may be a factor, and parameters such as the steadiness of the wind measured just above the water surface may be relevant.

Because of the obvious presence of surface films and because "if the wind changes its direction abruptly the streaks themselves are quickly reoriented (in a matter of one or two minutes only)," Stommel (1952) postulated that the phenomenon was essentially a shallow surface-layer effect and that the action of the film in damping capillary waves might be of importance for organizing the film into streaks. This postulate was taken up and explored by other authors, but it is now known that the windrows are the result of Langmuir circulations (LCs), organized longitudinal rolls with their axes parallel to the wind, and that surface films are not an integral part of the mechanism.

Since several scales of LCs may exist at any time (Faller and Caponi, 1978) the apparent rapid response of the windrows to wind variations may be presumed to be due primarily to the smaller scales, which are close to the surface and which respond more rapidly to changes in the wind. For example, in recent laboratory experiments with light wind Faller (1978) has found a characteristic growth rate of only 12 s for cells with a cross-wind wavelength of 44 cm. For larger scales one would certainly expect slower response times, but it now appears that reorganization of the pattern of surface streaks in a minute or two by the reformation of the LCs is not unreasonable.

I would now like to report some preliminary qualitative results on the generation of LCs in the presence of surface films. Figure 16.7 illustrates the wind-wave tank in which a regular pattern of crossed waves is generated and in which a wind is blown over the waves. In the absence of a finite-amplitude crossed-wave pattern and at low wind speeds there are virtually no wind waves generated over the working section of the tank, a length of about 5 m. In the presence of finite-amplitude crossed waves, however, the same air speed causes wind-generated waves of significant amplitude. From preliminary estimates it now appears that the large crossed waves and the smaller wind-generated waves both contribute to the growth of the observed LCs whose scale is determined by the crossed-wave pattern.

In previous papers (Faller, 1969; Faller and Caponi, 1978), it was reported that surface films completely prevented the formation of LCs, but this assertion must now be qualified on the basis of recent experiments. Of particular importance here is the effect of the finite length of the wind-wave tank, for this restricts the possible motion of the film. In light-wind conditions the wind stress will compress the surface film against the end of the tank, and a steady state is achieved when the internal film-pressure effect balances the wind stress. This condition can be avoided, at least temporarily, by introducing a surface film onto a clean water surface at the upwind end of the tank, for the film can then move downwind in response to the wind stress.

The effects of surface films under certain laboratory conditions can now be summarized as follows:

(1) Application of a surface film-forming material, in this case dodedyl alcohol, always damps wind-generated waves. Thus, whether moving or stationary, a film always destroys the contribution of small wind-generated waves to the LCs.

Table 16.1

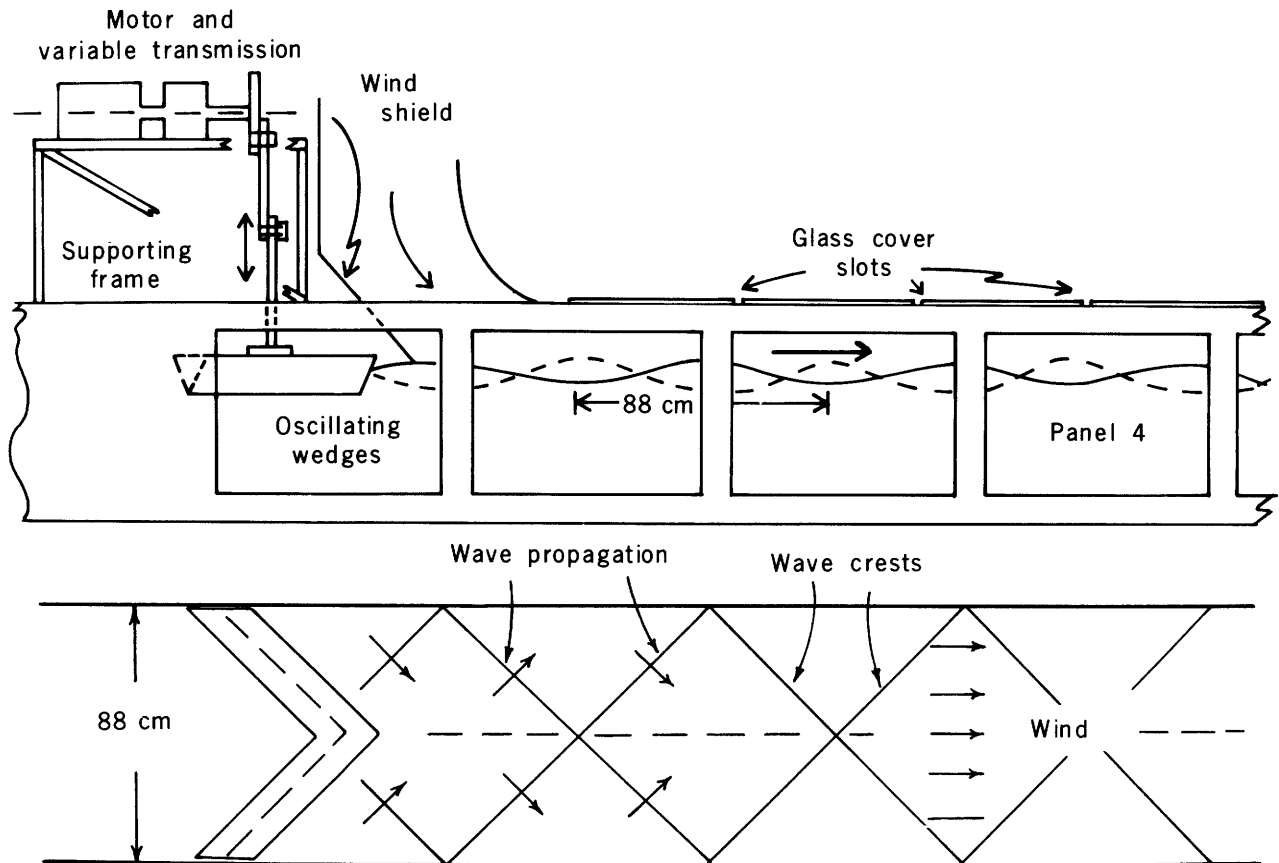| Wind speed (mph) | Number of observations | | |
	Streaks	No streaks	% streaks
<1.5	3	42	7
1.5–2.5	9	19	32
2.5–3.5	11	8	58
3.5–4.5	14	5	74
4.5–5.5	13	8	62
>5.5	54	3	95

Figure 16.7 Apparatus used for the generation of Langmuir circulations. The vertically oscillating wedges generate a crossed pattern of large waves that propagate along the length of the tank and are absorbed at the right-hand end. Wind is drawn in by an exhaust fan at the right-hand end to produce a shear flow in the water and small superimposed wind-generated waves.

(2) With the large, mechanically generated crossed waves present, LCs are not generated as long as the film is prevented from moving by compression against the end of the tank.

(3) With the same large waves present, LCs *are* generated if the surface film can move in response to the wind stress. In such a case, however, the wind-generated small waves are damped and do not contribute.

These observations lend additional support to the Craik-Leibovich theory of Langmuir circulations (Craik and Leibovich, 1976), which describes the action of essentially irrotational waves in twisting the vorticity of the wind-generated shear flow into the vorticity of the longitudinal rolls. Apparently the moving surface film can transmit the tangential wind stress to the water whereas the stationary film obviously cannot.

16.7 Concluding Remarks

From time to time one may have the impression that laboratory-model experiments have reached the limit of their usefulness—that all of the interesting and productive experiments have been performed, and that further experimentation will only be repetitious. Then too, many theories that formerly could only be tested in a physical-laboratory experiment can now be tested reliably with computer calculations. But from the extensive list of studies discussed above we perceive a gradual increase in the variety, sophistication, and application of laboratory experiments as novel experimental techniques are developed and as new theories emerge that isolate (abstract) interesting phenomena and require verification.

The laboratory experiments discussed in this review represent a necessarily restricted class of studies. Within this class, however, two progressions in style are evident: the first, from the attempts by von Arx to represent nature in detail insofar as possible, to experiments carefully matched to the corresponding theories and in which all aspects of the flow are analyzed in excruciating detail; the second, from the steady-state SAF experiments, through the transient spin-up, Rossby-wave, and oscillating-lid experiments, to the

Alan J. Faller

interaction of turbulence and the mean flow. The recent two-fluid experiments of Smith, Saunders, Whitehead, and Krishnamurti now seem to indicate a gradual progression from uniform-fluid models into the theoretically and technically more difficult realm of baroclinic models, and clearly it would be premature to conclude that there is no longer a role for laboratory studies. Indeed, as long as "no one believes a theory, except the theorist, and everyone believes an experiment—except the experimenter," the role of laboratory experiments in oceanographic research remains secure.